Journal of Human Genetics (2018) 63:297–307
https://doi.org/10.1038/s10038-017-0367-x

ARTICLE

GAREM1 regulates the PR interval on electrocardiograms

Hye Ok Kim[1] · Ji Eun Lim[1] · Myung Jun Kim[1] · Ji-One Kang[1] · Sung-Moon Kim[1] · Jeong Min Nam[1] · Jihoon Tak[2] · Hiroaki Konishi[3] · Tasuku Nishino[3] · In Song Koh[4] · Young-Ho Jin[5] · Hyung Hwan Baik[1] · Jin-Bae Kim[6] · Mi Kyung Kim[7] · Bo Youl Choi[7] · Sang-Hak Lee[8] · Yangsoo Jang[8] · Jinho Shin[9] · Bermseok Oh[1]

Received: 12 June 2017 / Revised: 22 August 2017 / Accepted: 6 September 2017 / Published online: 22 December 2017

Abstract

PR interval is the period from the onset of P wave to the start of the QRS complex on electrocardiograms. A recent genomewide association study (GWAS) suggested that *GAREM1* was linked to the PR interval on electrocardiograms. This study was designed to validate this correlation using additional subjects and examined the function of *Garem1* in a mouse model. We analyzed the association of rs17744182, a variant in the *GAREM1* locus, with the PR interval in 5646 subjects who were recruited from 2 Korean replication sets, Yangpyeong ($n = 2471$) and Yonsei ($n = 3175$), and noted a significant genomewide association by meta-analysis ($P = 2.39 \times 10^{-8}$). To confirm the function of Garem1 in mice, *Garem1* siRNA was injected into mouse tail veins to reduce the expression of *Garem1*. *Garem1* transcript levels declined by 53% in the atrium of the heart ($P = 0.029$), and *Garem1*-siRNA injected mice experienced a significant decrease in PR interval (43.27 ms vs. 44.89 ms in control, $P = 0.007$). We analyzed the expression pattern of Garem1 in the heart by immunohistology and observed specific expression of Garem1 in intracardiac ganglia. Garem1 was expressed in most neurons of the ganglion, including cholinergic and adrenergic cells. We have provided evidence that *GAREM1* is involved in the PR interval of ECGs. These findings increase our understanding of the regulatory signals of heart rhythm through intracardiac ganglia of the autonomic nervous system and can be used to guide the development of a therapeutic target for heart conditions, such as atrial fibrillation.

Introduction

Atrial fibrillation (AF) is a type of abnormal heart rhythm that is characterized by rapid and irregular beating, with a lifetime risk of development that ranges from 20 to 25% [1]. AF can be detected during a physical examination on an

Hye Ok Kim and Ji Eun Lim contributed equally to this work

Electronic supplementary material The online version of this article (https://doi.org/10.1038/s10038-017-0367-x) contains supplementary material, which is available to authorized users

✉ Yangsoo Jang
ohbs@khu.ac.kr

✉ Jinho Shin
jhs2003@hanyang.ac.kr

✉ Bermseok Oh
jangys1212@yuhs.ac

[1] Department of Biochemistry and Molecular Biology, School of Medicine, Kyung Hee University, 26, Kyunghee-daero, Dongdaemun-gu, Seoul 02447, Korea

[2] Department of Biomedical Science, Graduate School, Kyung Hee University, Seoul, Korea

[3] Faculty of Life and Environmental Sciences, Prefectural University of Hiroshima, Shobara, Hiroshima 727-0023, Japan

[4] Department of Physiology, College of Medicine, Hanyang University, Seoul, Korea

[5] Department of Physiology, School of Medicine, Kyung Hee University, Seoul, Korea

[6] Division of Cardiology, Kyung Hee University College of Medicine, Seoul, Korea

[7] Department of Preventive Medicine, College of Medicine, Hanyang University, Seoul, South Korea

[8] Division of Cardiology, Department of Internal Medicine, Severance Hospital and Cardiovascular Research Institute, Yonsei University College of Medicine, 250, Seongsanno, Seodaemun-gu, Seoul 03722, Korea

[9] Cardiology division, Department of Internal Medicine, Hanyang University, Medical Center, 222, Wangsimni-ro, Sungdong-gu, Seoul 04763, Korea

electrocardiogram (ECG), for which prolongation of PR interval is a risk factor [2]. PR interval is the period that extends from the sinoatrial node (SA node) to the ventricular myocardium, primarily through the atrioventricular node (AV node) [3]. ECG measurements are influenced by various mechanisms that involve several genetic and environmental factors, with ~50% heritability [4–6].

Recently, genome-wide association studies (GWASs) on ECGs have been performed in several ethnic groups, identifying many genetic loci [7–11]. In particular, five loci (*SCN5A-SCN10A, NKK2-5, CAV1/CAV2, SOX5*, and *TBX5*) have been reported to be associated with PR interval [7, 8, 12–14]. We have also conducted GWASs on ECGs in Korean and Japanese populations [15, 16], discovering a novel locus, rs17026156 (an *SLC8A1* variant), that correlates significantly with PR interval at $P < 5 \times 10^{-8}$ ($P = 2.58 \times 10^{-14}$). In addition, there is a potential association between rs17744182 in *GAREM1* and PR interval ($P = 6.25 \times 10^{-8}$) [15].

Garem1, Grb2-associated regulator of Erk/Mapk1, was originally identified as the tyrosine-phosphorylated protein FLJ21610 (or FAM59A) in phosphoproteomic studies on epidermal growth factor (EGF) signaling [17]. On stimulation of EGF, Garem1 is phosphorylated at 2 tyrosine residues (Tyr-105 and Tyr-453), becoming recognized by the SH3 domains of Grb2, and activates ERK/MAPK signaling in COS-7 and Hela cells [18]. No functional study has supported a link between Garem1 and PR interval.

In this study, to examine the genetic association between *GAREM1* and PR interval, we conducted two additional association analyses using 2471 Korean subjects from the Yangpyeong replication set and 3175 subjects from the Yonsei replication set and meta-analyzed the association results with previous findings. Further, to determine whether *Garem1* functions in PR interval, we measured the effects of *Garem1* silencing on ECG findings in mice and analyzed the expression pattern of Garem1 in mouse heart tissue.

Materials and methods

Subjects and ECG measurements

Our association analysis between PR interval and rs17744182 (a *GAREM1* variant) was performed in subjects aged 40–70 years, excluding those with concurrent use of medications, such as β-blockers, that interfered with ECG measurements. We also excluded subjects with myocardial infarction or any cerebrovascular accident in the past 3 months; significant arrhythmia, such as sinus node dysfunction, atrial fibrillation, and bundle branch; or atrioventricular block. Patients with pacing rhythm were also excluded.

The Yangpyeong study population has been described [19]. The Korean Multi-Rural communities Cohort Study (MRCohort) recruited subjects between 2005 and 2010 to examined risk factors for cardiovascular disease as a part of the Korean Genome Epidemiology Study (KoGES). We drew 3566 subjects from the Yangpyeong area (the eastern part of Gyeonggi-do province), for 3132 of whom genotype data were available. After applying the exclusion criteria, 2471 subjects were ultimately included for this analysis.

The Yonsei replication set comprised 3807 subjects who participated in baseline health examinations for a community-based cohort study in Seoul between April 2010 and November 2012. Of them, 3175 subjects met the inclusion criteria and were used for this analysis.

PR interval values were obtained from a supine 12-lead ECG using digital electrocardiographic recorders: an FCP-2101 (Fukuda Denshi Co.) for the Yangpyeong replication set and a MAC 2000 (General Electric Healthcare, Milwaukee, Wisconsin, USA) for the Yonsei replication set. PR interval was measured for the period from the onset of P wave to the onset of ventricular depolarization. Ultimately, the ECG signals were reviewed by cardiologists.

Basic clinical parameters, such as weight, height, and blood pressure, were measured in both replication sets (Yangpyeong and Yonsei) using standard protocols. Written informed consent was obtained from all Yangpyeong study subjects, and study project was approved by the institutional review board of the Korea National Institute of Health. And the Yonsei study subjects were withdrawn from Cardiovascular Genome Center Cohort, Yonsei University College of Medicine, Korea and the Institutional Review Board of Severance Hospital approved the study protocol.

Genotyping and imputation

The genotype data for the Yangpyeong replication set were generated using the Korean Chip (K-CHIP), which was designed by the Center for Genome Science, Korea National Institute of Health (KNIH), based on the UK Biobank Axiom® Array, and manufactured by Affymetrix (Santa Clara, CA, USA). The genotype quality control criteria were as follows: genotype call rate > 0.95, minor allele frequency (MAF) > 0.01, and Hardy–Weinberg equilibrium ($P > 1 \times 10^{-6}$); related individuals were excluded by computing pairwise identity-by-state values. SNP imputation was performed with IMPUTE2 [20] using Phase 1 of the 1000 Genomes Project as a reference panel. Variants with an INFO score > 0.8 and MAF > 0.01 were retained for analysis. The total number, gone through the procedure of genotype quality control were 7,734,874

SNPs, and the genotype data of rs17744182 SNP among them was extracted and used for the association analysis.

The rs17744182 SNP was genotyped in Yonsei replication subjects using a TaqMan probe assay, and the fluorescence level of PCR products was measured on a 7900HT Fast Real-Time PCR System (Applied Biosystems, Foster, CA, USA).

Animal research and ethics statement

All BALB/c mice (Japan SLC, Inc., Shizuoka, Japan) were used at age 7–9 weeks for the experiments. They were housed and handled in a pathogen-free facility in the College of Pharmacy at Kyung Hee University per the Guide for the Care and Use of Laboratory Animals. The mice were maintained on a 12-h light/dark cycle at a constant temperature with free access to food (LabDiet 5L79, St. Louis, MO, USA) and water. Every effort was made to minimize the number of killed animals and their suffering. Animals were anesthetized by intraperitoneal (i.p.) injection of tribromoethanol (Avertin, 18 ml of working solution per kg body weight), the working solution of which was diluted to 25 µg/ml in 0.9% NaCl from a stock solution (1 g/ml 2,2,2, tribromoethanol dissolved in tertiary amyl alcohol), and killed by cervical dislocation after the experimental procedure. The experiment was approved by the local committee for the Care and Use of Laboratory Animals, Kyung Hee University (license number: KHUASP(SE)-16-036).

In vivo delivery of *Garem1* siRNA

The selection and in vivo delivery of siRNA have been described [21–23]. In brief, 5 *Garem1* siRNAs were synthesized by Genolution (Seoul, Korea), 1 of which was selected for injection into mouse tail veins. To determine their silencing efficacy, 20 nM of the siRNAs was transfected into NIH3T3 cells using Lipofectamine 2000 (Invitrogen, Carlsbad, CA, USA) per the manufacturer's instructions. TRP53 siRNA was used as a positive control for the in vitro transfection experiment. The *Garem1* siRNA and scrambled control siRNA sequences are shown in Supplementary Table 1.

For in vivo delivery into mice, a polyethylenimine compound, in vivo-jetPEI™ (Polyplus, 201-10G, Illkirch-Graffenstaden, France), was used as the transfection reagent. On the basis of the manufacturer's instructions, 50 µg of siRNA and 6.5 µl of in vivo-jetPEI (N/P charge ratio of 6) were diluted with 50 µl 10% glucose solution and 50 µl sterile H_2O. The solution was vortexed gently and left for 15 min at room temperature. The mixture was injected into the tail veins of 7–9-week-old BALB/c mice, and 6 h later, the treated mice were used for experiments, such as electrocardiography measurements, collection of tissues for mRNA quantitation, and western blot.

ECG measurement and data analysis

The ECG protocol has been described [24]. ECGs were recorded using a computerized data acquisition and analysis system. Mice (7–9 weeks, female, 20–25 g) were anesthetized with tribromoethanol (Avertin, 18 ml of working solution per kg body weight), as described above. After complete induction of anesthesia (< 3 min), acupuncture needle (DB106; 0.20×15 mm; DongBang Acupuncture, Inc., Sungnam, Korea) electrodes were inserted subcutaneously according to the lead II ECG scheme (into the right forelimb and both hind limbs) (Supplementary Fig. 1). The diaphragm signal was amplified through a bridge amplifier and recorded on a PowerLab system (LabChart 7, AD Instruments, Bella Vista, Australia). The mean values for heart rate, PR, P wave, QRS duration, QT, and RR interval were calculated from the ECG data for each mouse, which were collected for 5 min. The PR segment was obtained by subtracting the P wave length from the PR interval, and the QTc interval was the value that was corrected by the heart rate according to Bazett's formula ($QTc = QT/(RR)^{0.5}$, RR interval = 60/heart rate) [25]. The ECG signals were reviewed by a cardiologist.

Quantitative real-time PCR

Total RNA was extracted from mouse tissues using TRIzol (Invitrogen, Carlsbad, CA, USA). complementary DNA (cDNA) was synthesized from 500 ng of total RNA using the PrimeScript™ RT kit (TaKaRa, Shiga, Japan) per the manufacturer's protocol. Quantitative real-time PCR analysis was performed using SYBR Green I (TaKaRa, Shiga, Japan) on an ABI Step One Real-Time PCR system (Applied Biosystems, Foster, CA, USA) using the following program: 45 cycles at 95 °C for 10 s, 60°C for 15 s, and 72 °C for 20 s. The following primer sequences were used: forward, 5′-AAGCCCCACCCTGTCTTACT-3′, reverse, 5′-AGGACTTCCAAATGGGGACT-3′. The data were expressed as the average relative mRNA level in each group. Relative mRNA expression was calculated as follows: the Ct value of *Gapdh* was subtracted from that of *Garem1*, and the delta Ct (ΔCt) value was converted to the linear term $2-\Delta Ct$.

Western blot

Total proteins were extracted from mouse tissues using PRO-PREP protein extraction solution (Intron Biotechnology, Gyeonggi-Do, Korea) per the manufacturer's instructions. Protein concentrations were measured by Bradford assay [26]. Total proteins (10 to 40 µg) were separated by 8–10% SDS–PAGE and transferred to a nitrocellulose membrane (Pall, Ann Arbor, MI, USA). The membrane was

blocked in 5% skim milk for 30 min at room temperature and subsequently incubated with antibody overnight at 4 °C (Supplementary Table 2). The blot was then incubated with horseradish peroxidase-conjugated secondary antibody (Santa Cruz Biotechnology, Inc., Santa Cruz, CA, USA) for 1 h at room temperature. Protein signals were detected using Luminol (Santa Cruz Biotechnology, Inc., Santa Cruz, CA, USA) and exposed to x-ray films (Agfa-Health Care NV, Mortsel, Belgium). Relative band densities were determined using ImageJ (v.1.46) [27], and total proteins were normalized to actin.

Immunohistochemistry

To detect our proteins of interest by immunohistochemistry, mouse heart tissue (7–9-week-old, male, 20–25 g) was harvested and fixed with 4% paraformaldehyde in phosphate-buffered saline, pH 7.4 for 24 h. The tissue was dehydrated in a series of ethanols and xylene and embedded in paraffin. Tissue sections (4-μm thickness) were prepared on a Leica RM2125 microtome (Leica Biosystems, Nussloch, Germany) and hydrated in xylene and a series of ethanols. After deparaffinization and rehydration, the sections were immersed for 15 min in methanol that contained 3% hydrogen peroxide to block endogenous peroxidase activity. All slides were pretreated with citrate buffer (10 mM; pH 6.0) for antigen retrieval by heating the slides in a microwave oven at 97°C for 20 min. A cooling period of 20 min preceded the incubation with the primary antibody.

Following a blocking step in Protein Block Serum-Free solution (Dako, California, USA), the specimens were incubated with a primary antibody (Supplementary Table 2) overnight at 4 °C. Then, the EnVision™ system (Dako, California, USA) was used to stain per the manufacturer's instructions. All stains were developed with diaminobenzidine. Before the slides were mounted, all sections were counterstained for 1 min with hematoxylin and dehydrated in alcohol and xylene. The stained slides were observed under a Nikon Eclipse Ci upright microscope (Tokyo, Japan).

For immunofluorescence, antigen-retrieved tissue sections, as described above, were blocked in 2.5% normal horse serum (Vector Laboratories, Burlingame, CA, USA) and incubated with primary antibody overnight at 4 °C. The primary antibodies are listed in Supplementary Table 2. The sections were then incubated with VectaFluorTM Ready-to-Use DyLight dye-labeled secondary antibody (DyLight 594 Goat Anti-Rabbit IgG; DyLight 488 Goat Anti-Goat IgG; Vector Laboratories, Burlingame, CA, USA) and mounted using VectaShield Mounting Media with DAPI (Vector Laboratories). Images were acquired with a ZEISS LSM 700 confocal microscope (ZEN 2012 LE, Oberkochen, Germany).

Statistical analysis

The association between the *GAREM1* variant and PR interval were analyzed by linear regression, adjusted for age, sex, recruitment area, BMI, systolic blood pressure, and height. A meta-analysis of the association results of this study and previous findings was performed by inverse-variance method under the assumption of fixed effects using Cochran's Q test to determine between-study heterogeneity [28]. All statistical analyses were performed in PLINK v1.09 [29]. A forest plot for a meta-analysis of 5 PR interval association studies was constructed using R, version 3.2.0.

All data between case and control groups were analyzed by Mann–Whitney U-test, because it is generally considered to be more powerful than the *t*-test [30]. The statistical analysis was performed using SPSS (PASW Statistics 22.0). The number of mice that were used for each group is noted in the parentheses in the figures. All data were reported as mean ± SEM. $P < 0.05$ was considered to be statistically significant.

Table 1 Clinical characteristics of subjects

Variables	Previous report[a]			Replication analysis	
	KARE	Japanese 1	Japanese 2	Yangpyeong	Yonsei
n (% male)	6805 (50.4%)	2285 (31.9%)	5010 (33.3%)	2471 (35.8%)	3175 (30.7%)
Age (years)	51.6 (8.7)	49.8 (13.9)	56.7 (13.4)	57.2 (8.4)	59.2 (6.8)
BMI (kg/m^2)	24.6 (3.1)	22.2 (3.2)	22.6 (3.2)	24.8 (3.1)	24.7 (2.9)
SBP (mm Hg)	116.4 (17.9)	120.1 (16.8)	126.1 (19.1)	122.0 (16.6)	119.0 (14.5)
Height (cm)	160.6 (8.7)	160.4 (8.3)	158.6 (8.7)	158.4 (8.2)	159.2 (7.8)
PR interval (ms)	163.2 (35.9)	158.1 (21.4)	158.7 (22.0)	167.1 (22.3)	166.5 (21.3)

Data are presented as mean (standard deviation)

BMI body mass index, *SBP* systolic blood pressure

[a]Hong et al. [15]

Results

GAREM1 is associated with PR interval

To determine whether the *GAREM1* locus is associated with PR interval, two additional association analyses were performed in 2471 Korean subjects from the Yangpyeong replication set and 3175 subjects from the Yonsei replication set.

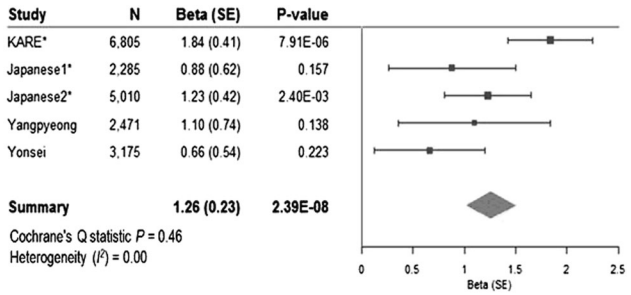

Fig. 1 Forest plot of the meta-analysis of rs17744182 using five PR interval association analyses Forest plot shows the study-specific association results (Beta (SE)) for three previous studies (marked by *) and the two new studies, presented as boxes and bars. The contribution of each study to the meta-analysis is indicated by the size of the square. The result of the meta-analysis of the five analyses is shown as a diamond (Hong et al. [15]). A full color version of this figure is available at the *Journal of Human Genetics* journal online.

The clinical characteristics of the subjects in the new association studies and three earlier reports are described in Table 1. rs17744182, located in the first intron of *GAREM1*, was examined in the linear regression model as an independent variable of PR interval, controlling for age, sex, body mass index, systolic blood pressure, and height as covariates.

The association *P*-values between rs17744182 and PR interval did not pass the level of significance in Yangpyeong ($P = 0.138$) and Yonsei ($P = 0.223$) set. However, the meta-analysis of the five association studies, including three previous reports, showed a significant genome-wide association ($\text{beta} \pm \text{SE} = 1.26 \pm 0.23$, $P = 2.39 \times 10^{-8}$). The forest plots of rs17744182 in each study are shown in Fig. 1.

Silencing of *Garem1* decreases PR interval

To confirm the function of *Garem1* in PR interval, we silenced this gene by injecting siRNA into mice, as described [21–23]. Five *Garem1* siRNAs were synthesized and tested for their silencing efficacy in NIH3T3 cells, and the most effective siRNA (Supplementary Table 1) was selected for in vivo injection. The siRNA was mixed with polyethylenimine and injected into mouse tail veins. Then, we measured *Garem1* mRNA levels 6 h later by quantitative

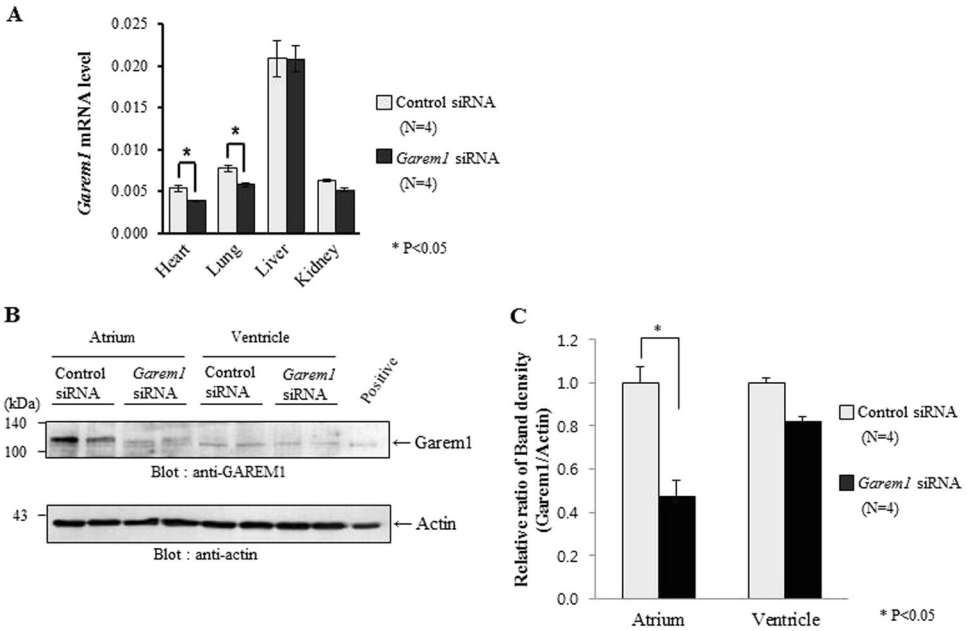

Fig. 2 Decrease in mRNA and protein expression of Garem1 siRNA-injected mice. **a** Decrease in mRNA in *Garem1* siRNA-injected mouse tissues. The relative expression of mRNA in each tissue is presented as the fold-change in relative mRNA levels in mice 6 h after injection with control siRNA and *Garem1* siRNA. **b** Reduction of protein expression in heart tissue of *Garem1* siRNA-injected mice. Garem1 levels in atrium and ventricle tissue are shown for siRNA-injected mice by western blot. The positive control was prepared from lysates from NIH3T3 cells transfected with Garem1 cDNA plasmid (kindly provided by Professor Hiroaki Konish), with actin as the loading control. **c** Garem1 protein levels in atrium and ventricle are presented as the average of 4 independent protein band densities from siRNA-injected mice. Number in parentheses indicates the pair number of mice used for real-time PCR **A** and western blot **c**. Error bars show the mean ± SEM. *P* values were calculated by Mann–Whitney U-test. $^*P < 0.05$ vs. respective controls

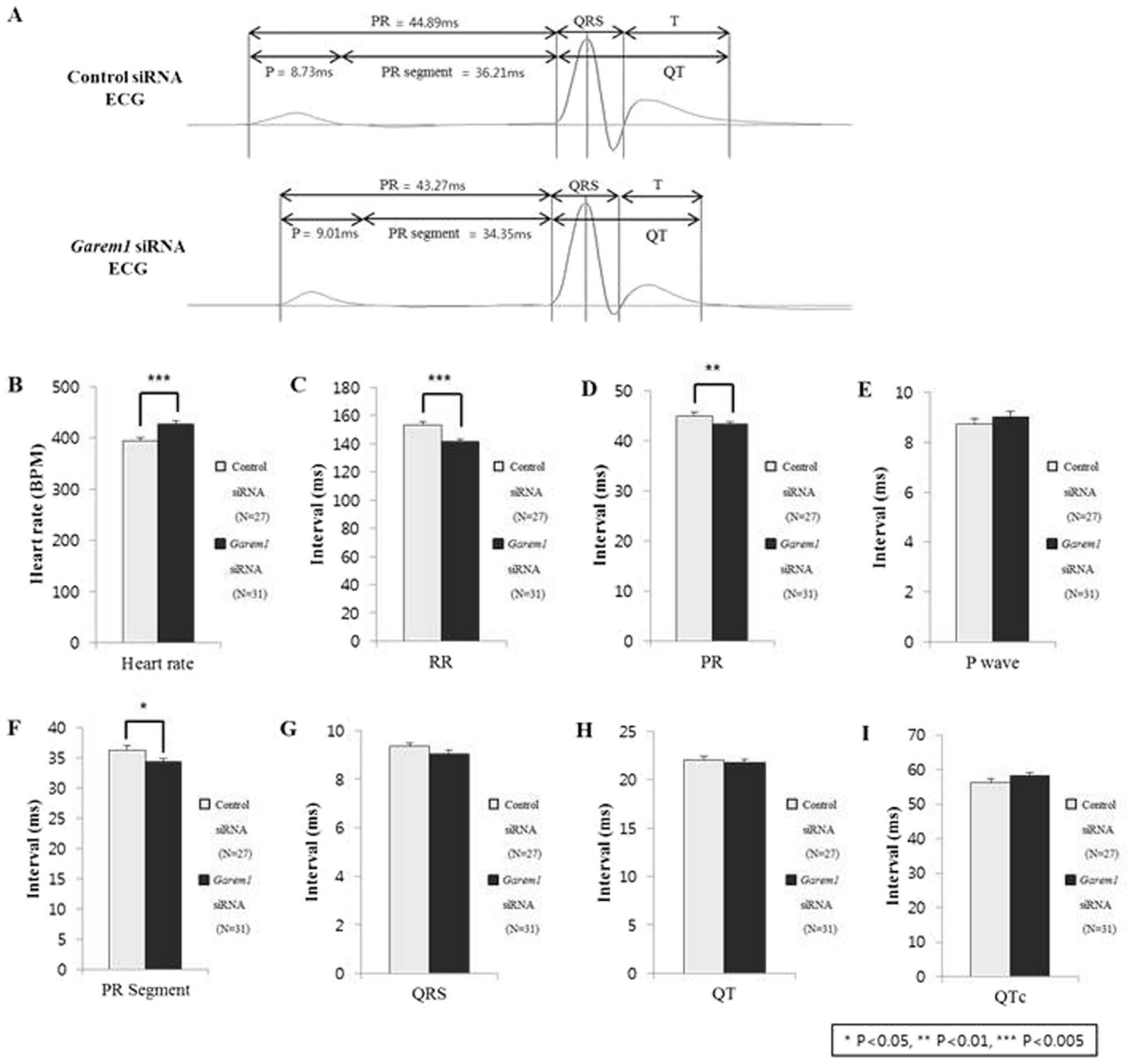

Fig. 3 Decrease in PR interval in *Garem1* siRNA-injected mice. **a** Representative ECG signal 6 h after *Garem1* siRNA (lower) and control siRNA (upper) injection in mice. The values are the average PR, P wave, and PR segment. **b–i** Comparison of each ECG value between *Garem1* siRNA-injected mice and control. The bar graphs show the mean ECG recordings for heart rate, RR interval, PR interval, P wave, PR segment, QRS duration, QT interval, and QTc interval for each group. Error bars show the mean ± SEM. *P* values were calculated by Mann–Whitney U-test. $^{*}P < 0.05$, $^{**}P < 0.01$, $^{***}P < 0.005$ vs. respective controls

real-time PCR, comparing them between *Garem1* siRNA- and control siRNA-injected mice. *Garem1* mRNA levels decreased significantly in heart by 27% ($P < 0.05$, control siRNA $N = 4$ and *Garem*1 siRNA $N = 4$) and in lung by 25% ($P < 0.05$, control siRNA $N = 4$ and *Garem1* siRNA $N = 4$), although they did not change significantly in liver or kidney (Fig. 2a).

We also performed western blot using the atrium and ventricle of the heart. Garem1 expression in the atrium was higher than in the ventricle in normal mice and declined significantly in the atrium on injection of *Garem1* siRNA (53% in atrium, $P = 0.029$ and 18% in ventricle, $P = 0.114$) (Fig. 2b, c).

To estimate the change in cardiac conduction on siRNA injection, an ECG was taken from *Garem1*-siRNA mouse. *Garem1* siRNA-injected mice had a significantly lower RR interval (141.25 vs. 153.49 ms in control, $P = 0.001$, control siRNA $N = 27$ and *Garem1* siRNA $N = 31$) and PR interval (43.27 vs. 44.89 ms in control, $P = 0.007$, control siRNA $N = 27$ and *Garem1* siRNA $N = 31$) and increased heart

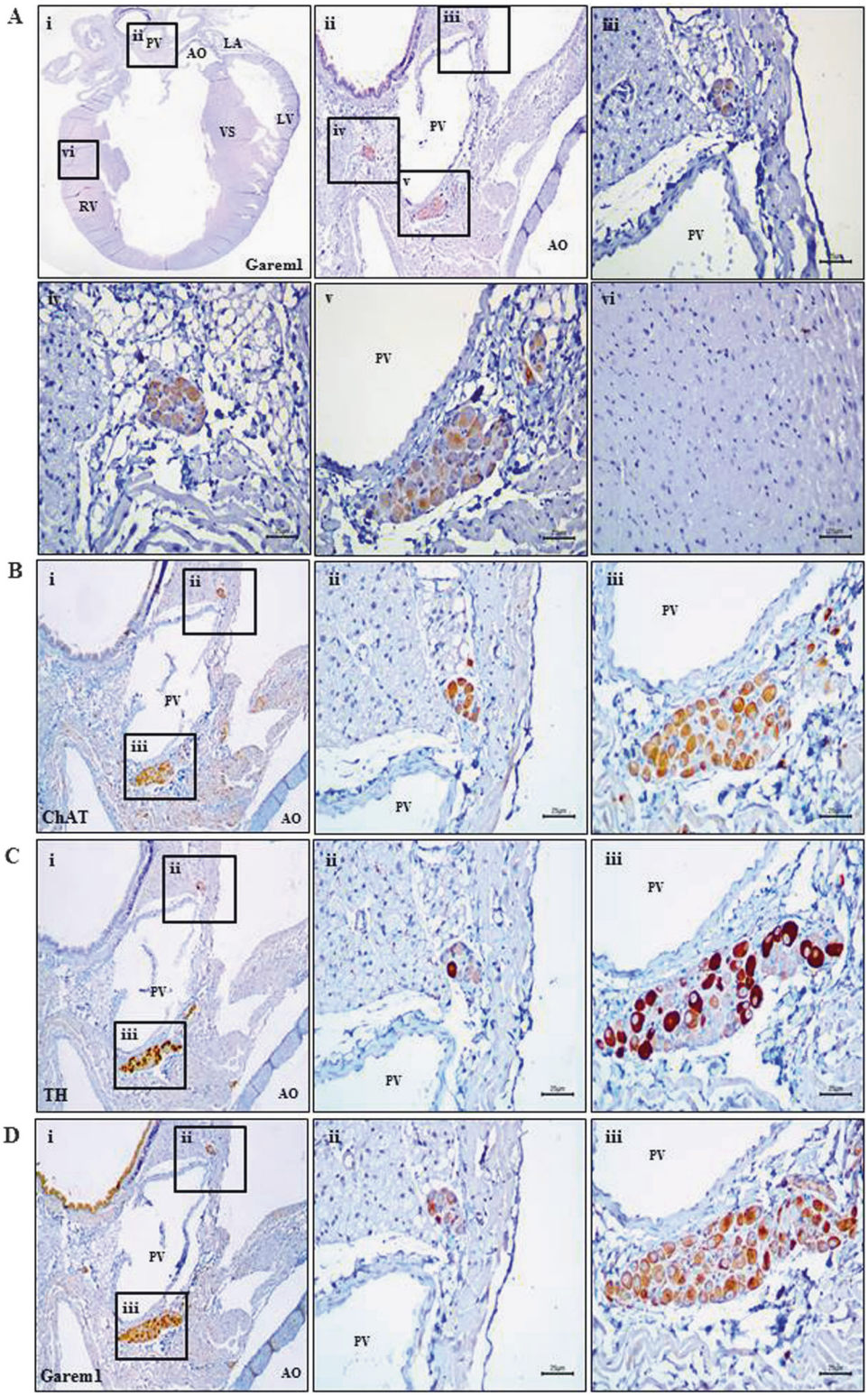

Fig. 4 Immunohistochemical staining of Garem1 and neuronal markers (ChAT and TH) in cardiac ganglion of normal mice **a** Garem1 immunostaining (brown) in heart tissue of normal mice. The ganglia in the box (ii) are located in atrial adipose tissue. Garem1-positive cells reside in the cardiac ganglion neighboring the pulmonary vein region (**a**-iii to **a**-v). To provide detailed views of each ganglion, the box (ii) in **a**-i is enlarged in **a**-ii, and the boxes (iii, iv, v) in **a**-ii are enlarged in **a**-iii, **a**-iv, and **a**-v, respectively. The ventricle was tested as a negative control (**a**-vi). **b** Choline acetyltransferase (ChAT) immunostaining in cardiac ganglion. ChAT is a marker of parasympathetic neural cells. **c** Tyrosine hydroxylase (TH) immunostaining in cardiac ganglion. TH is a marker of sympathetic neural cells. **d** Garem1 immunostaining in a serial slide to **b** and **c**. The panels (**a**-iii, iv, v, vi and **b**, **c**, **d**-ii, iii) are shown in a highly magnified view (scale bars: 25 μm). *PV* pulmonary vein, *LA* left atrium, *LV* left ventricle, *VS* ventricular septum, *RV* right ventricle, *AO* aorta

rate (426.82 vs. 393.51 bpm in control, $P = 0.002$, control siRNA $N = 27$ and *Garem1* siRNA $N = 31$).

The PR interval consists of the P wave and PR segment, as shown in Fig. 3a. We then examined which component of the PR interval was altered by *Garem1* silencing in the ECGs. We noted a significant decrease in PR segment (34.35 vs. 36.21 ms in control, $P = 0.011$, control siRNA $N = 27$ and *Garem1* siRNA $N = 31$) compared with control groups but not in the length of the P wave (Fig. 3b–i). The PR segment corresponds to the period in which electric

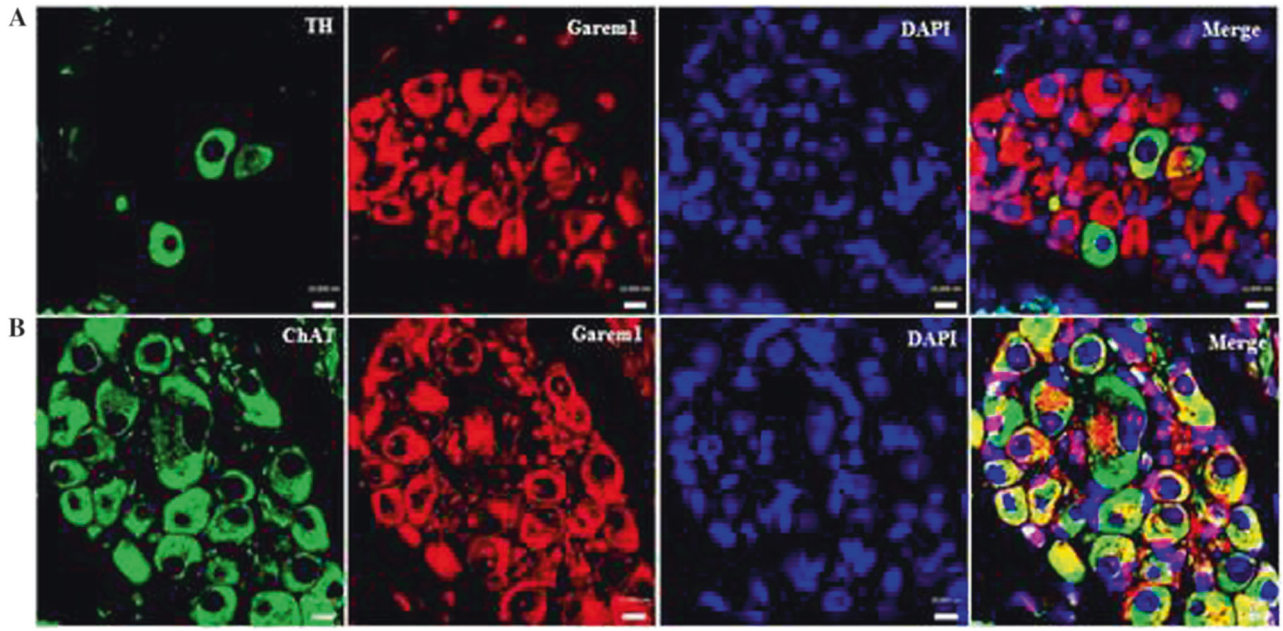

Fig. 5 Colocalization of Garem1 and neuronal markers (ChAT or TH) in cardiac ganglion of normal mice In the cardiac ganglion, Garem1 staining overlaps with neuronal markers. **a** Most Garem1-positive neurons (red) stain for ChAT (green), indicating that most Garem1-expressing neurons are of cholinergic origin. **b** Few Garem1-positive cells (red) show TH (green) staining

signals are delayed at the AV node, before they travel through the ventricular branches to induce cardiac depolarization [31]. Fig. 3a shows representative ECG diagrams in *Garem1* and control siRNA-injected mice.

Garem1 protein is expressed in intracardiac ganglia of the atrium

Because the SA and AV nodes reside in the atria and because more Garem1 is expressed in the atria compared with the ventricle, we studied the expression pattern of Garem1 in mouse heart tissue by immunohistochemistry. Notably, Garem1 was specifically expressed in cardiac ganglia, which influence sinus and atrioventricular nodal function. As shown in Fig. 4a, Garem1 protein was stained within intracardiac ganglia in adipose tissue that was adjacent to the pulmonary vein. The intracardiac ganglia that are involved in neural control of the heart comprise cholinergic (parasympathetic) and adrenergic (sympathetic) neurons [32]. Choline acetyltransferase (ChAT) and tyrosine hydroxylase (TH) are markers of parasympathetic and sympathetic elements, respectively. On the basis of these neuronal markers, we confirmed that the Garem1-positive region is consistent with cardiac ganglia, including ChAT- and TH-positive cells (Fig. 4b, c).

To examine the expression of Garem1 in adrenergic and cholinergic neurons, we analyzed the ganglia by immunofluorescence (Fig. 5). Garem1 was simultaneously expressed in cholinergic and adrenergic cells. Notably, ChAT-positive (cholinergic) ganglion cells were more abundant than TH-positive (adrenergic) cells in cardiac ganglia.

Discussion

GAREM1 is involved in the regulation of the PR interval on an ECG, as evidenced by the following: the association between rs17744182 in *GAREM1* and PR interval, the change in PR interval in *Garem1* siRNA-injected mice, and the specific expression of Garem1 in intracardiac ganglia.

Heart rhythm on an ECG is largely regulated by the cardiac autonomic nervous system (ANS) [32]. The autonomic innervation of the heart involves the extrinsic and intrinsic cardiac ANSs [33]. The intrinsic cardiac ANS is a complex network that is composed of ganglionated plexi (GP) that are concentrated within epicardial fat pads. GP serves as "integration centers" that modulate the connection between the extrinsic (vagosympathetic and sympathetic trunk) and intrinsic (ganglionated plexi) cardiac ANSs in the regulation of heart rhythm [34–38]. Cardiac GP are also critical in the initiation and maintenance of AF. Several clinicians have demonstrated that AF can be eliminated by ablating GP [39–41]. In our study, the specific expression of Garem1 in cardiac GP suggests that GAREM1 is one of molecules that modulate the activity of the cardiac ANS in cardiac GP [18].

Intrinsic cardiac GP contain parasympathetic and sympathetic neural elements [42]. Clinical and experimental

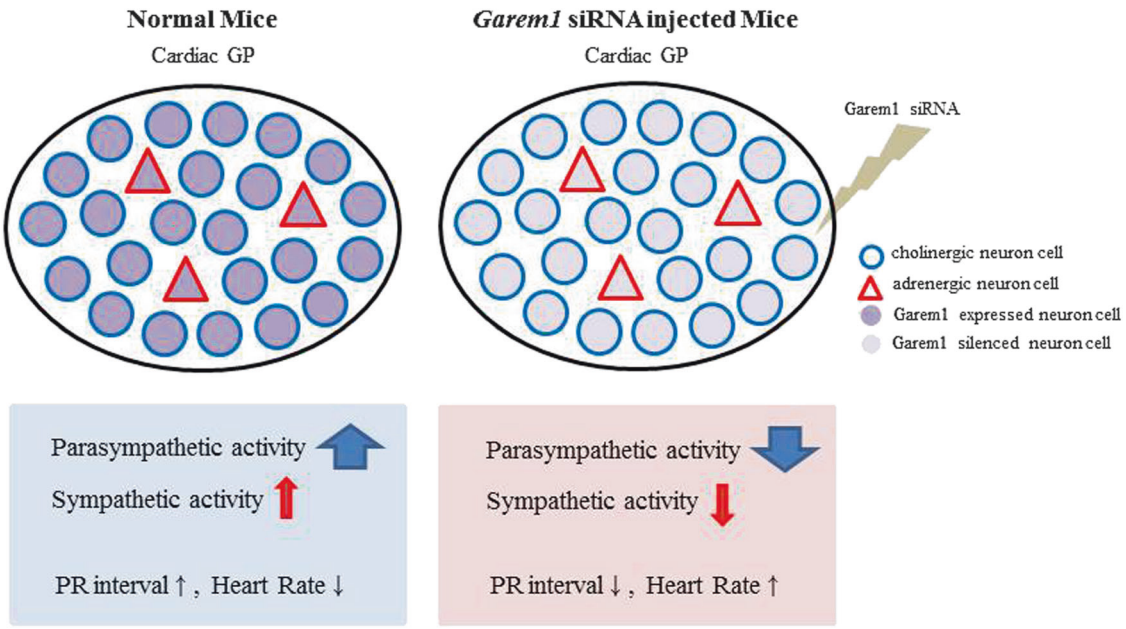

Fig. 6 Diagram of the potential function of Garem1 in intracardiac ganglionated plexi The blue circle expresses domination of cholinergic cells, whereas the red triangle indicates the small number of adrenergic cells within cardiac GP. In normal mice, Garem1 protein is expressed in most cells of the ganglion. In *Garem1* siRNA-injected mice, the low level of Garem1 predominantly decreases parasympathetic activity due to the large number in the ganglion. As a result, heart rate is enhanced and PR interval is reduced

studies have proposed that the balance between cholinergic (parasympathetic) and adrenergic (sympathetic) cardiac inputs is important for the regulation of heart rhythm [37]. In addition, Petraitiene et al. reported that the distribution of adrenergic and cholinergic fibers in intrinsic nerves differs, depending on the intracardiac location of GP [43]. By histology, Jiang et al. showed that ChAT-positive ganglion (parasympathetic) cells and TH-positive ganglion (sympathetic) cells are contained in the GP of dogs, the former of which were more abundant [44]. Their observation is consistent with our findings, and because Garem1 is expressed in cholinergic and adrenergic cells, most Garem1-positive neurons reside in cells of cholinergic origin in the mouse GP.

As a novel adaptor in EGF receptor signaling, Garem1 has been shown to be related to the activation of Erk in non-neuronal cells [18, 45, 46]. Erk activation also occurs in several neuronal cells that are stimulated by neurotransmitters, including acetylcholine, glutamate, and dopamine [47, 48], and MAPKs, including Erk, are important regulators of several neuronal functions, such as survival [49], differentiation [50], and synaptic plasticity [51]. The mechanism that underlies the regulation of heart rhythm through Garem1 is unknown. However, we speculate that Garem1 in cardiac GP affects heart rhythm by delivering signals from extrinsic neurons to the SA or AV node via the adrenergic/cholinergic receptor-mediated signal transduction pathway. This hypothesis can be tested using Garem1 knockout mice—preferably a cardiac ganglion-specific knockout line—to determine the function of Garem1 in adrenergic or cholinergic receptor-mediated signaling.

Another hypothesis is that Garem1 functions similarly in sympathetic and parasympathetic neurons in the cardiac ganglion, but the effects of Garem1 appear to be more robust on parasympathetic activity, due to the abundance of cholinergic neurons in cardiac ganglion. Figure 6 depicts a model of cardiac GP in *Garem1* siRNA-injected mice. Under normal conditions, parasympathetic activity is greater than sympathetic activity in GP, because cholinergic cells predominate over adrenergic cells in them. However, in *Garem1*-siRNA treated mice, Garem1 levels decrease in both types of cells in GP, resulting in a greater decline in parasympathetic activity relative to sympathetic activity, shortening the PR interval and increasing heart rate.

The limitation of this study includes the absence of experimental evidence that supports the implication of the sequence variant rs17744182 in the expression of *GAREM1*. The experiment requires human cardiac tissue, sample of which we have not obtained yet. However, based on a bioinformatic in silico analysis, rs17744182 might functions in the expression of *GAREM1*. According to the ENCODE database (www.encodeproject.org), rs17744182 is related to a histone modification and a transcription factor-binding motif. Moreover, although there are no eQTL data on this SNP in the Genotype-Tissue Expression (GTEx) database (www.gtexportal.org), rs60451418, located ~28 kb from rs17744182, regulates *GAREM1* expression in lung tissue, and these SNPs are in linkage disequilibrium ($r^2 = 0.65$).

The second limitation of this study is the lack of an examination of general circulation in *Garem1* siRNA-injected mice. Therefore, we cannot exclude the possibility that the changes in heart rate and PR interval in our mice were influenced by fluctuations in general circulation, such as blood pressure, in addition to the direct effect of Garem1 on ECG through cardiac GP.

In this study, we have demonstrated that rs17744182 in *GAREM1* is associated with PR interval on an ECG with genomewide significance ($P=2.39\times10^{-8}$) by a meta-analysis of five studies, that silencing of *Garem1* in mice reduces PR interval, and that Garem1 is specifically expressed in intracardiac ganglia. These findings suggest that *GAREM1* regulates heart rhythm by modulating cardiac GP function, implicating it as a novel target for the treatment of heart diseases, including AF.

Acknowledgements This work was supported by the National Research Foundation of Korea (NRF) grant funded by the Korea government (MSIP) (nos. 2014R1A2A2A01005277 and 2015R1C1A2A01052431). Genotype data were produced using the Korean Chip (K-CHIP) available through the K-CHIP consortium. K-CHIP was designed by Center for Genome Science, Korea National Institute of Health, Korea (4845-301, 3000-3031).

Compliance with Ethical Standards

Conflict of interests The authors declare no competing financial interests.

References

1. Heeringa J, van der Kuip DA, Hofman A, Kors JA, van Herpen G, Stricker BH, et al. Prevalence, incidence and lifetime risk of atrial fibrillation: the Rotterdam study. Eur Heart J. 2006;27:949–53.
2. Ferguson C, Inglis SC, Newton PJ, Middleton S, Macdonald PS, Davidson PM, et al. Atrial fibrillation: stroke prevention in focus. Aust Crit Care. 2014;27:92–8.
3. Smith JG, Lowe JK, Kovvali S, Maller JB, Salit J, Daly MJ, et al. Genome-wide association study of electrocardiographic conduction measures in an isolated founder population: Kosrae. Heart Rhythm. 2009;6:634–41.
4. DeFilippis AP, Larned JM, Cole JH, Nell-Dybdahl C, Miller JI, Sperling LS. Clues to cardiovascular risk: an office-based approach. Prev Cardiol. 2007;10:36–41.
5. Milan DJ, Lubitz SA, Kaab S, Ellinor PT. Genome-wide association studies in cardiac electrophysiology: recent discoveries and implications for clinical practice. Heart Rhythm. 2010;7:1141–8.
6. Schwartz PJ, Wolf S. QT interval prolongation as predictor of sudden death in patients with myocardial infarction. Circulation. 1978;57:1074–7.
7. Pfeufer A, van Noord C, Marciante KD, Arking DE, Larson MG, Smith AV, et al. Genome-wide association study of PR interval. Nat Genet. 2010;42:153–9.
8. Holm H, Gudbjartsson DF, Arnar DO, Thorleifsson G, Thorgeirsson G, Stefansdottir H, et al. Several common variants modulate heart rate, PR interval and QRS duration. Nat Genet. 2010;42:117–22.
9. Sotoodehnia N, Isaacs A, de Bakker PI, Dorr M, Newton-Cheh C, Nolte IM, et al. Common variants in 22 loci are associated with QRS duration and cardiac ventricular conduction. Nat Genet. 2010;42:1068–76.
10. Pfeufer A, Sanna S, Arking DE, Muller M, Gateva V, Fuchsberger C, et al. Common variants at ten loci modulate the QT interval duration in the QTSCD Study. Nat Genet. 2009;41:407–14.
11. Newton-Cheh C, Eijgelsheim M, Rice KM, de Bakker PI, Yin X, Estrada K, et al. Common variants at ten loci influence QT interval duration in the QTGEN Study. Nat Genet. 2009;41:399–406.
12. Chambers JC, Zhao J, Terracciano CM, Bezzina CR, Zhang W, Kaba R, et al. Genetic variation in SCN10A influences cardiac conduction. Nat. Genet. 2010;42:149–52.
13. Smith JG, Magnani JW, Palmer C, Meng YA, Soliman EZ, Musani SK, et al. Genome-wide association studies of the PR interval in African Americans. PLoS Genet. 2011;7:e1001304.
14. Butler AM, Yin X, Evans DS, Nalls MA, Smith EN, Tanaka T, et al. Novel loci associated with PR interval in a genome-wide association study of 10 African American cohorts. Circ Cardiovasc Genet. 2012;5:639–46.
15. Hong KW, Lim JE, Kim JW, Tabara Y, Ueshima H, Miki T, et al. Identification of three novel genetic variations associated with electrocardiographic traits (QRS duration and PR interval) in East Asians. Hum Mol Genet. 2014;23:6659–67.
16. Kim JW, Hong KW, Go MJ, Kim SS, Tabara Y, Kita Y, et al. A common variant in SLC8A1 is associated with the duration of the electrocardiographic QT interval. Am J Hum Genet. 2012;91:180–4.
17. Blagoev B, Ong SE, Kratchmarova I, Mann M. Temporal analysis of phosphotyrosine-dependent signaling networks by quantitative proteomics. Nat Biotechnol. 2004;22:1139–45.
18. Tashiro K, Tsunematsu T, Okubo H, Ohta T, Sano E, Yamauchi E, et al. GAREM, a novel adaptor protein for growth factor receptor-bound protein 2, contributes to cellular transformation through the activation of extracellular signal-regulated kinase signaling. J Biol Chem. 2009;284:20206–14.
19. Choi S, Jung S, Kim MK, Shin J, Shin MH, Shin DH, et al. Gene and dietary calcium interaction effects on brachial-ankle pulse wave velocity. Clin Nutr. 2016;35:1127–34.
20. Howie BN, Donnelly P, Marchini J. A flexible and accurate genotype imputation method for the next generation of genome-wide association studies. PLoS Genet. 2009;5:e1000529.
21. Park SY, Lee HJ, Ji SM, Kim ME, Jigden B, Lim JE, et al. ANTXR2 is a potential causative gene in the genome-wide association study of the blood pressure locus 4q21. Hypertens. Res. 2014;37:811–7.
22. Shin YB, Lim JE, Ji SM, Lee HJ, Park SY, Hong KW, et al. Silencing of Atp2b1 increases blood pressure through vasoconstriction. J Hypertens. 2013;31:1575–83.
23. Ji SM, Shin YB, Park SY, Lee HJ, Oh B. Decreases in Casz1 mRNA by an siRNA complex do not alter blood pressure in mice. Genomics Inform. 2012;10:40–3.
24. Kim MJ, Lim JE, Oh B. Validation of non-invasive method for electrocardiogram recording in mouse using lead II. Biomed Sci Lett. 2015;21:1–9.
25. Mitchell GF, Jeron A, Koren G. Measurement of heart rate and Q-T interval in the conscious mouse. Am J Physiol. 1998;274: H747–51.
26. Gotham SM, Fryer PJ, Paterson WR. The measurement of insoluble proteins using a modified Bradford assay. Anal Biochem. 1998;173:353–8.
27. Schneider CA, Rasband WS, Eliceiri KW. NIH Image to ImageJ: 25 years of image analysis. Nat Methods. 2012;9:671–5.
28. Ioannidis JP, Patsopoulos NA, Evangelou E. Heterogeneity in meta-analyses of genome-wide association investigations. PLoS ONE. 2007;2:e841.
29. Purcell S, Neale B, Todd-Brown K, Thomas L, Ferreira MA, Bender D, et al. PLINK: a tool set for whole-genome association

and population-based linkage analyses. Am J Hum Genet. 2007;81:559–75.
30. Fay MP, Proschan MA. Wilcoxon-Mann-Whitney or t-test? On assumptions for hypothesis tests and multiple interpretations of decision rules. Stat Surv. 2010;4:1–39.
31. Ariyarajah V, Prajapat L, Kumar KK, Barac I, Apiyasawat S, Spodick DH. Quantitative estimation of left atrial linear dimension on a transthoracic echocardiogram using an electrocardiographic formulaic assessment. Am J Cardiol. 2007;100:894–8.
32. Rimmer K, Harper AA. Developmental changes in electrophysiological properties and synaptic transmission in rat intracardiac ganglion neurons. J Neurophysiol. 2006; 95:3543–52.
33. Pauza DH, Skripka V, Pauziene N. Morphology of the intrinsic cardiac nervous system in the dog: a whole-mount study employing histochemical staining with acetylcholinesterase. Cells Tissues Organs. 2002;172:297–320.
34. Hou Y, Scherlag BJ, Lin J, Zhang Y, Lu Z, Truong K, et al. Ganglionated plexi modulate extrinsic cardiac autonomic nerve input: effects on sinus rate, atrioventricular conduction, refractoriness, and inducibility of atrial fibrillation. J Am Coll Cardiol. 2007;50:61–8.
35. Hou Y, Scherlag BJ, Lin J, Zhou J, Song J, Zhang Y, et al. Interactive atrial neural network: determining the connections between ganglionated plexi. Heart Rhythm. 2007;4:56–63.
36. Kapa S, Venkatachalam KL, Asirvatham SJ. The autonomic nervous system in cardiac electrophysiology: an elegant interaction and emerging concepts. Cardiol Rev. 2010;18:275–84.
37. Klein HU, Ferrari GM. Vagus nerve stimulation: A new approach to reduce heart failure. Cardiol J. 2010;17:638–44.
38. Katritsis DG. Autonomic denervation for the treatment of atrial fibrillation. Indian Pacing Electrophysiol J. 2011;11:161–6.
39. Hwang C, Wu TJ, Doshi RN, Peter CT, Chen PS. Vein of marshall cannulation for the analysis of electrical activity in patients with focal atrial fibrillation. Circulation. 2000;101:1503–5.
40. Chen SA, Tai CT. Catheter ablation of atrial fibrillation originating from the non-pulmonary vein foci. J Cardiovasc Electrophysiol. 2005;16:229–32.
41. Lin WS, Tai CT, Hsieh MH, Tsai CF, Lin YK, Tsao HM, et al. Catheter ablation of paroxysmal atrial fibrillation initiated by non-pulmonary vein ectopy. Circulation. 2003;107:3176–83.
42. Po SS, Nakagawa H, Jackman WM. Localization of left atrial ganglionated plexi in patients with atrial fibrillation. J Cardiovasc Electrophysiol. 2009;20:1186–9.
43. Petraitiene V, Pauza DH, Benetis R. Distribution of adrenergic and cholinergic nerve fibres within intrinsic nerves at the level of the human heart hilum. Eur J Cardiothorac Surg. 2014;45:1097–105.
44. Cui B, Lu Z, He B, Hu X, Wu B, Xu S, et al. Acute effects of ganglionated plexi ablation on sinoatrial nodal and atrioventricular nodal functions. Auton Neurosci. 2011;161:87–94.
45. Taniguchi T, Tanaka S, Ishii A, Watanabe M, Fujitani N, Sugeo A, et al. A brain-specific Grb2-associated regulator of extracellular signal-regulated kinase (Erk)/mitogen-activated protein kinase (MAPK) (GAREM) subtype, GAREM2, contributes to neurite outgrowth of neuroblastoma cells by regulating Erk signaling. J Biol Chem. 2013;288:29934–42.
46. Nishino T, Matsunaga R, Konishi H. Functional relationship between CABIT, SAM and 14-3-3 binding domains of GAREM1 that play a role in its subcellular localization. Biochem Biophys Res Commun. 2015;464:616–21.
47. Kanno H, Horikawa Y, Hodges RR, Zoukhri D, Shatos MA, Rios JD, et al. Cholinergic agonists transactivate EGFR and stimulate MAPK to induce goblet cell secretion. Am J Physiol Cell Physiol. 2003;284:C988–98.
48. Rosenblum K, Futter M, Jones M, Hulme EC, Bliss TV. ERKI/II regulation by the muscarinic acetylcholine receptors in neurons. J. Neurosci. 2000;20:977–85.
49. Fukunaga K, Miyamoto E. Role of MAP kinase in neurons. Mol Neurobiol. 1998;16:79–95.
50. Cowley S, Paterson H, Kemp P, Marshall CJ. Activation of MAP kinase kinase is necessary and sufficient for PC12 differentiation and for transformation of NIH 3T3 cells. Cell. 1994;77:841–52.
51. English JD, Sweatt JD, A requirement for the mitogen-activated protein kinase cascade in hippocampal long term potentiation. J Biol Chem.1997;272:19103–6